

RSC Advances



This is an *Accepted Manuscript*, which has been through the Royal Society of Chemistry peer review process and has been accepted for publication.

Accepted Manuscripts are published online shortly after acceptance, before technical editing, formatting and proof reading. Using this free service, authors can make their results available to the community, in citable form, before we publish the edited article. This *Accepted Manuscript* will be replaced by the edited, formatted and paginated article as soon as this is available.

You can find more information about *Accepted Manuscripts* in the [Information for Authors](#).

Please note that technical editing may introduce minor changes to the text and/or graphics, which may alter content. The journal's standard [Terms & Conditions](#) and the [Ethical guidelines](#) still apply. In no event shall the Royal Society of Chemistry be held responsible for any errors or omissions in this *Accepted Manuscript* or any consequences arising from the use of any information it contains.



RSC advances

ARTICLE

An electrochemical sensor based on DNA polymerase and HRP-SiO₂ nanoparticles for the ultrasensitive detection of K-ras gene point mutation

Received 00th January 20xx,

Chengfei Zhao^a, Feng Gao^d, Shaohuang Weng^b, Qicai Liu^{*,c}, Liqing Lin^{*,b} and Xinhua Lin^b

Accepted 00th January 20xx

DOI: 10.1039/x0xx00000x

www.rsc.org/

We successfully developed an electrochemical DNA sensor for the precise detection of K-ras gene point mutation. The proposed sensor was based on DNA replication, which fully employed the 5'→3' polymerization activity of DNA polymerase I and the principle of base pairing. The biotin-dUTP only linked with the base A, instead of base G. And then, the streptavidin-HRP-SiO₂ nanoparticles combining with the biotin-dUTP on the modified electrode produced the current signal in the TMB solution. The streptavidin-HRP-SiO₂ nanoparticles had the effect of amplified signal. Hence, the sensitivity and selectivity of the proposed sensor were observably enhanced, comparison with the previously reported DNA sensors. The response current of the amperometric i-t curve of the prepared sensor showed a good linear correlation with the logarithm of target DNA concentration in the range from 0.001 pM to 1000 pM with the limit of detection of 0.42 fM. And the current value was also proportional to the logarithm of target DNA concentration from 0.01 pM to 100 pM when the hybridization solution contained other mutant K-ras genes and wild K-ras gene. Thus, this proposed approach provided the good basis and a promising platform that the mutant K-ras gene in the clinical genomic sample can be directly detected.

Introduction

Pancreatic cancer is a common malignancy with poor prognosis because of its aggressive disease. Pancreatic cancer is associated with the high mortality rate and one of the top five causes of cancer death [1]. Although diagnostic techniques of cancer have received a rapid development, only about 4% of patients with pancreatic cancer live five years after diagnosis, and pancreatic cancer poorly responds to most chemotherapeutic agents [2]. Unfortunately, there is no remarkable early symptom in pancreatic cancer progresses [3]. Most patients with pancreatic cancer are always in middle-late stage when diagnosed, and meanwhile cancer cell metastasis has occurred. At this time pancreatic cancer can not be already cured. At present, the surgical removal of tumor at early stage is only an effective means to cure pancreatic cancer [4]. Thus, early detection technologies of pancreatic cancer will directly

influence the cure of the disease and the quality of life in patients, and can prolong the patient survival [5].

The study found that the process of histopathologic lesions of pancreatic cancer is from normal pancreatic duct to pancreatic intraepithelial neoplasia (PanIN) [6], which was divided into three stages, such as PanIN-1, PanIN-2 and PanIN-3 [2]. Each stage was associated with genovariation at the molecular level [7]. The point mutations of K-ras gene was believed to be "early" genetic mutation, which occurred in pancreatic duct lesions with minimal atypia, namely PanIN-1 [8]. The study showed that 52.2% of pancreatic cancers were found to have a point mutation of K-ras gene, and most mutations of K-ras gene occurred at condon 12 where 57.7% of point mutations were GGT to GAT [9], implying K-ras gene can act as gene marker of pancreatic cancer. Point mutations of K-ras gene can be used to monitor and diagnose pancreatic cancer [10]. So, in order to curb the high mortality rates from pancreatic cancer, it is necessary to develop a convenient and efficient method for the detection of point mutations of K-ras gene.

At present, although there have been several methods for the detection of point mutations of DNA [11-14], inherent disadvantages restrict those methods to be widely applied in clinical. However, electrochemical biosensing technologies have unique advantages, such as high sensitivity, easy operation and lower cost, so electrochemical biosensors are paid more and more attention, especially electrochemical DNA sensors that were developed to detect specific DNA sequence. According to the requirements of clinical test, including easy operation, quick response, high sensitivity and low cost, we

^a Pharmaceutical and Medical Technology College, Putian University, Putian 351100, China.

^b Department of Pharmaceutical Analysis, Faculty of Pharmacy, Fujian Medical University, Fuzhou 350108, China.

^c Department of Clinical Laboratory, The First Affiliated Hospital of Fujian Medical University, Fuzhou 350005, China

^d Department of Pathology, The First Affiliated Hospital of Fujian Medical University, Fuzhou 350005, China

* Corresponding author: Liqing Lin: fjmu_lin@126.com; Qicai Liu: lqc673673673@163.com.

† Footnotes relating to the title and/or authors should appear here. Electronic Supplementary Information (ESI) available: Table S1 and Fig. S1. See DOI: 10.1039/x0xx00000x

developed a novel electrochemical DNA sensor based on DNA polymerase I and streptavidin horseradish peroxidase (streptavidin-HRP) modified SiO₂ nanoparticles for the accurate detection of point mutation of K-ras gene. Amperometric i-t curve was used to record the current signal. The working principle and manufacturing process of DNA sensor are shown in Fig. 1. Briefly, the captured DNA with -SH was immobilized on the surface of the prepared Au electrode (AuE) by the interaction of Au-S. After that, the 6-mercapto-1-hexanol (MCH) was employed to take over the blank space of the modified AuE and orientate the captured DNA fixed on AuE. When the target DNA hybridized with the captured DNA on AuE at suitable temperature, the mutation site of target DNA flushed with the free-end of captured DNA. And then, DNA polymerase I with 5'→3' polymerization activity was employed to connect biotin-dUTP with mutation site of target DNA. Because the detection sites of wild K-ras gene and target DNA were respectively GGT and GAT, and the biotin-dUTP strictly matched with base A, instead of base G, the biotin-dUTP only linked with the detection site of target DNA (base A) by DNA polymerase I. However, the biotin-dUTP didn't react with the detection site of wild K-ras gene (base G) or other mutant K-ras genes (base T or C). The target DNA linking with biotin-dUTP would bond with streptavidin-HRP modified SiO₂ nanoparticles through biotin-streptavidin interaction. In the detection solution containing TMB, the catalytic reaction of HRP on the modified AuE was employed to produce electrochemical signal that was recorded by amperometric i-t curve, and the electrochemical signal was proportional to the amount of target DNA.

In our work, we successfully applied the enzymology principles and nanometer materials. Details are as follows: ① the principle of base pairing and 5'→3' polymerization activity of DNA polymerase I improved the selectivity and specificity of the proposed electrochemical DNA sensor; ② streptavidin-HRP modified SiO₂ nanoparticles markedly amplified the electrochemical signal to enhance the sensitivity of the sensor; ③ the HRP has efficient catalytic properties for TMB substrate to make the electrochemical signal more stable. Therefore, the target DNA was precisely detected in strict biochemical reaction.

In this study, the proposed approach could be well employed to detect the target DNA. Because of aiming at single-base mutation, the approach can be used for the research of single nucleotide polymorphisms and the detection of single base mutations. More importantly, due to the unique advantages of the electrochemical DNA sensor, the approach will have promising application.

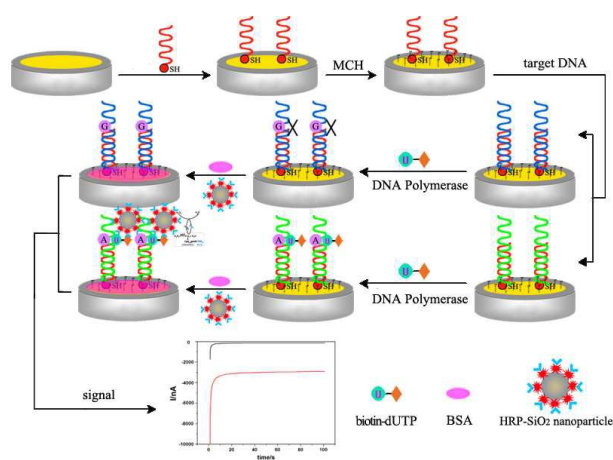


Fig. 1 Schematic diagram of the proposed electrochemical DNA sensor for the detection of target DNA.

Materials and methods

Chemicals and materials

All the oligonucleotide sequences and DNA polymerase I were purchased from Takara Biotechnology Co., Ltd (Dalian, China). The biotin-dUTP and streptavidin-horseradish peroxidase (HRP) were purchased from Roche Diagnostics GmbH (Penzberg, Germany). 3,3',5,5'-tetramethylbenzidine (TMB) substrate (K-blue low activity substrate) was from Neogen (Lansing, MI, USA). Bovine serum albumin (BSA) was from Sigma-Aldrich (St Louis, MO, USA). The DNA sequences are listed as follow:

Captured DNA: 5'-(SH C6)AAAAAAGGCACTCTTGCCTACGCCA-3'

Mutant K-ras gene (target DNA): 5'-CTTGTGGTAGTTGGAGCTGATGGCGTAGGCAAGAGTGCCT-3'

Mutant K-ras gene (non-target DNA 1): 5'-CTTGTGGTAGTTGGAGCTGTTGGCGTAGGCAAGAGTGCCT-3'

Mutant K-ras gene (non-target DNA 2): 5'-CTTGTGGTAGTTGGAGCTGCTGGCGTAGGCAAGAGTGCCT-3'

Wild K-ras gene: 5'-CTTGTGGTAGTTGGAGCTGGTGGCGTAGGCAAGAGTGCCT-3'

Ethylenediamine tetraacetic acid (EDTA), potassium ferrocyanide trihydrate (K₄[Fe(CN)₆]•3H₂O), potassium ferricyanide (K₃[Fe(CN)₆]), cyclohexane, n-hexanol, Triton X-100, tetraethoxysilane, absolute ethyl alcohol, Tris(hydroxymethyl)methyl aminomethane (Tris), NH₃•H₂O, NaOH, NaCl, HCl, H₂SO₄, Na₂HPO₄•10H₂O and NaH₂PO₄•2H₂O were purchased from Sinopharm Chemical Reagent Co. Ltd (Shanghai, China). These reagents were of analytical reagent grade. Alumina powder was obtained from AlfaAesar (USA). 6-mercapto-1-hexanol (MCH) and γ-glycidioxypropyltrimethoxysilane (γ-GPMS) was obtained from Sigma-Aldrich (St Louis, MO, USA). The ultrapure water with a specific resistance of 18.2 MΩ•cm was prepared with Milli-Q-purified system (Billerica, MA, USA). Au electrode (AuE) (Φ=2

mm) was obtained from Shanghai ChenHua Instruments Co (China).

Phosphate buffer solution (PBS, pH=7.4) acted as the hybridization buffer containing 100 mM NaH_2PO_4 - Na_2HPO_4 and 100 mM NaCl and its pH was adjusted with 50 mM H_3PO_4 solution and NaOH solution. TE buffer (pH=8.0) was used to dilute the captured DNA, containing 10 mM Tris, 1.0 mM EDTA and 1 M NaCl, and pH of the solution was adjusted with 50 mM HCl. All the experimental solution was stored in a refrigerator (4 °C) when not used.

Preparation of SiO_2 nanoparticles

According to the previous report with some modification, SiO_2 nanoparticles were prepared by the reverse micelle method [15]. The specific steps were as follows: 10 mL of cyclohexane, 2 mL of n-hexanol and 2 mL of Triton X-100 were mixed and continuously stirred for 10 min; 450 mL of deionized water were then added into the mixture, and the above mixture was continuously stirred for 30 min to get a water-in-oil microemulsion; 200 μL of tetraethoxysilane and 100 μL of 25% $\text{NH}_3 \cdot \text{H}_2\text{O}$ (V/V) were slowly dropped into the microemulsion with continuously stirring to get the reaction mixture; After stirring for 24 h at room temperature, about 5 mL of ethanol was added into the reaction mixture to make the microemulsion break up; Next, the mixture was centrifuged with 3000 rpm for 15 min and washed three times with ethanol and deionized water, respectively; The final products were freeze-dried in vacuum, and then stored at 4 °C when not used.

Streptavidin horseradish peroxidase modified SiO_2 nanoparticles

Streptavidin horseradish peroxidase (streptavidin-HRP) was immobilized on the surface of SiO_2 nanoparticles by the amine-epoxy interaction. 0.05 g of dry SiO_2 nanoparticles was firstly dispersed in 5 mL of dry toluene. After the solution was sonicated for 2 h, 1% γ -GPMs (V/V) was added into the solution. After the solution was shook for 2 h, the epoxy groups were modified on the surface of the SiO_2 nanoparticles. The nanoparticles with epoxy groups were successively washed with dry toluene, acetone and ethanol, and then dispersed in 5 mL of PBS with pH 7.4. When not used, the solution was stored at 4 °C. 500 μL of 1 mg/mL streptavidin-HRP was added into the suspension of SiO_2 nanoparticles with epoxy groups. After the mixture was stirred at 4 °C for 12 h, unbound streptavidin-HRP was removed through rinsing with PBS (pH=7.4) three times. Finally, the SiO_2 nanoparticles with streptavidin-HRP were treated with 500 μL of 1% BSA (V/V) for 24 h to block any residual epoxy groups on the surface of SiO_2 nanoparticles. After centrifuged and washed with PBS (pH=7.4) three times, the streptavidin-HRP modified SiO_2 nanoparticles were obtained, and then dispersed in 5 mL of PBS with pH 7.4, namely HRP- SiO_2 nanoparticles. When not used, the solution was stored at 4 °C.

Pretreatment of Au electrode

The untreated Au electrode (AuE) was polished with alumina powder suspension of 0.3 μm and 0.05 μm in sequential order on microcloth pad, and then was adequately washed by ultrasonic cleaning in HNO_3 solution (HNO_3 : H_2O =1:1), absolute ethyl alcohol and double distilled water for 5 min, respectively. After the polished AuE was dried with nitrogen, it was electrochemically cleaned to remove any residuum by cyclic voltammetry in 10 mL of the fresh H_2SO_4 solution (0.5 M) [16].

Preparation of electrochemical DNA sensor

A 2 μL of captured DNA solution (1 μM) was gently dropped on a treated AuE. The AuE was kept for 1 h at 25 °C to immobilize the captured DNA by the interaction of Au-S. After thoroughly rinsed with PBS (pH=7.4) and double distilled water in proper order, the modified AuE was immersed in a 100 μL of MCH with 1 mM for 1 h at 25 °C to take over the blank space of the AuE and orientated the captured DNA fixed on the AuE, which decreased the nonspecific adsorption, made subsequent hybridization reaction easier and lessen the background signal. After thoroughly rinsed with PBS (pH=7.4) and double distilled water successively, the modified AuE was acted as ssDNA/MCH/AuE.

The ssDNA/MCH/AuE hybridized with a series of different concentrations target DNA for 1 h at 50 °C to obtain dsDNA/MCH/AuE. After thoroughly rinsed with PBS (pH=7.4) and double distilled water successively, 3 μL of mixed solution containing biotin-dUTP and DNA polymerase I was dropped on the modified AuE surface at 37 °C for 1 h to form dUTP/dsDNA/MCH/AuE. After being rinsed as the above method, the modified AuE was immersed in 200 μL of 0.5% BSA at 25 °C for 1 h to obtain BSA/dUTP/dsDNA/MCH/AuE. After thoroughly rinsed with PBS (pH=7.4) and double distilled water, 5 μL of HRP- SiO_2 nanoparticles solution was dropped on the above modified AuE at 37 °C for 15 min. The HRP- SiO_2 nanoparticles linked with the biotin-dUTP by the reaction of biotin-streptavidin system to obtain HRP/BSA/dUTP/dsDNA/MCH/AuE. 0.5% BSA could decrease the nonspecific adsorption of HRP- SiO_2 nanoparticles on the modified AuE to lower the background signal.

Electrochemical measurements

A conventional three-electrode system composing of the work electrode (modified AuE), reference electrode (Ag/AgCl electrode) and auxiliary electrode (platinum wire) was used for all the electrochemical detections. The amperometric i-t curve (namely i-t curve) and cyclic voltammetry (CV) were performed on an Autolab PGSTAT302F system (Eco Chemie, The Netherlands) in 500 μL of TMB solution. Electrochemical impedance spectroscopy (EIS) was carried out on an Autolab PGSTAT302F system in 10 mL of the fresh test solution containing 10 mM $[\text{Fe}(\text{CN})_6]^{3-}/[\text{Fe}(\text{CN})_6]^{4-}$ and 1 M KCl. The images of transmission electron microscopy (TEM) and scanning electron microscope (SEM) were obtained with a

JEOL JEM-1400 Microscope and a Hitachi S-4800 SEM system, respectively.

Results and discussion

Morphology characterization of bare SiO₂ nanoparticles and HRP-SiO₂ nanoparticles

The morphology of bare SiO₂ nanoparticles and HRP-SiO₂ nanoparticles were examined via scanning electron microscope (SEM) and transmission electron microscope (TEM). Fig. 2 showed TEM images and SEM images. The diameter of bare SiO₂ nanoparticles (Fig. 2A) was about 30 nm and revealed acceptable monodispersity, which resulted in the large surface area of SiO₂ nanoparticles. After streptavidin-HRP modified SiO₂ nanoparticles, HRP-SiO₂ nanoparticles showed obvious shade in Fig. 2B. The diameter of HRP-SiO₂ nanoparticles clearly increased to about 40 nm. Fig. 2C depicted that the surface of bare SiO₂ nanoparticles was very smooth. The surface of HRP-SiO₂ nanoparticles in Fig. 2D was significantly rough and had distinct attachments. These results illustrated that a large amount of streptavidin-HRP wrapped SiO₂ nanoparticles.

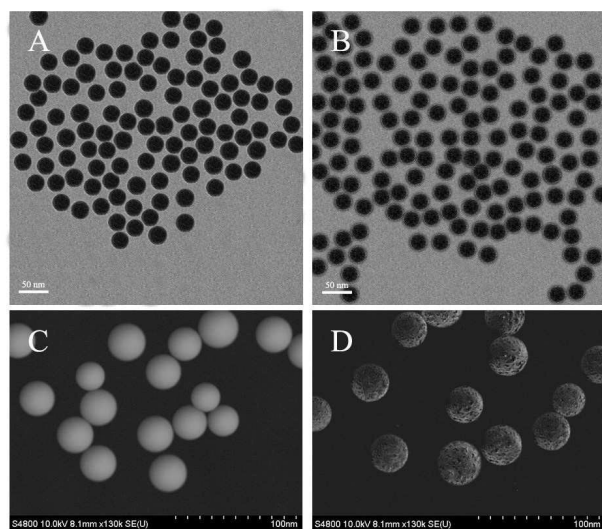


Fig. 2 TEM images of bare SiO₂ nanoparticles (A) and HRP-SiO₂ nanoparticles (B); SEM images of bare SiO₂ nanoparticles (C) and HRP-SiO₂ nanoparticles (D)

Electrochemical characterization of different modified electrodes

Electrochemical impedance spectroscopy (EIS) and cyclic voltammetry (CV) were performed to provide the interfacial properties of the modified AuE in different stages. Fig. 3A showed that the Nyquist plots of EIS consisted of a semicircle part and a linear part. The semicircle part at high frequencies corresponded with the electron transfer resistance, and the linear part at low frequencies corresponded with the diffusion process. The insert in Fig. 3A displayed the equivalent

electrical circuit of the work electrode, Ret of which was the electron transfer resistance of the work electrode interface, R_s of which represented the solution resistance, C_d of which represented the double layer capacitance and Z_w of which was Warburg impedance, respectively.

The EIS of bare AuE showed a nearly straight line (curve a) and the Ret was almost 0, indicating that there was nothing on bare AuE. After the self-assembly of captured DNA and MCH were orderly on AuE, the EIS evidently appeared semicircle part, the Ret of which (namely ssDNA/AuE and ssDNA/MCH/AuE) was about 1000 Ω (curve b) and 2200 Ω (curve c), respectively, implying captured DNA and MCH were successfully immobilized on the AuE surface to make Ret increase. After target DNA hybridized on the modified AuE to form dsDNA/MCH/AuE, the Ret greatly increased to be about 4800 Ω (curve d), suggesting that target DNA successfully hybridized with the captured DNA on AuE to form double-stranded DNA. The double-stranded DNA carried a large number of negative charges to hinder [Fe(CN)₆]³⁻/[Fe(CN)₆]⁴⁻ diffusion to the modified electrode surface. The Ret value further increased to be about 5900 Ω (curve e) after the reaction of biotin-dUTP, namely dUTP/dsDNA/MCH/AuE, meaning the biotin-dUTP successfully linked with base A by DNA polymerase I. After the modified AuE was sealed with 0.5% BSA, BSA being protein molecules of nonconductor would go against the electron transfer on the modified AuE surface and made the Ret of BSA/dUTP/dsDNA/MCH/AuE increase to be about 9200 Ω (curve f). Finally, the Ret value of HRP-SiO₂/BSA/dUTP/dsDNA/MCH/AuE reached to 11000 Ω (curve g) after HRP-SiO₂ nanoparticles reacted with biotin-dUTP on the modified AuE.

Fig. 3B showed CV of different modified electrodes. CV of bare AuE (curve a) had a pair of nearly reversible redox peaks, and the current of the redox peaks was maximum. The redox peak current of CV of ssDNA/AuE (curve b) and ssDNA/MCH/AuE (curve c) successively decreased, and the potential difference of the redox peaks successively increased. As the hybridization went on, the current of the redox peaks of dsDNA/MCH/AuE (curve d) and dUTP/dsDNA/MCH/AuE (curve e) further reduced in sequence, and the reversibility of the redox peaks was from bad to worse. Next, the redox current of BSA/dUTP/dsDNA/MCH/AuE (curve f) and HRP-SiO₂/BSA/dUTP/dsDNA/MCH/AuE (curve g) all cut down once again, meanwhile the reversibility was rather worse. The result of the redox current in Fig. 3B gradually reducing was obviously consistent with the Ret gradually increasing in Fig. 3A. The results of EIS and CV adequately suggested that it was successful to modify the AuE step by step.

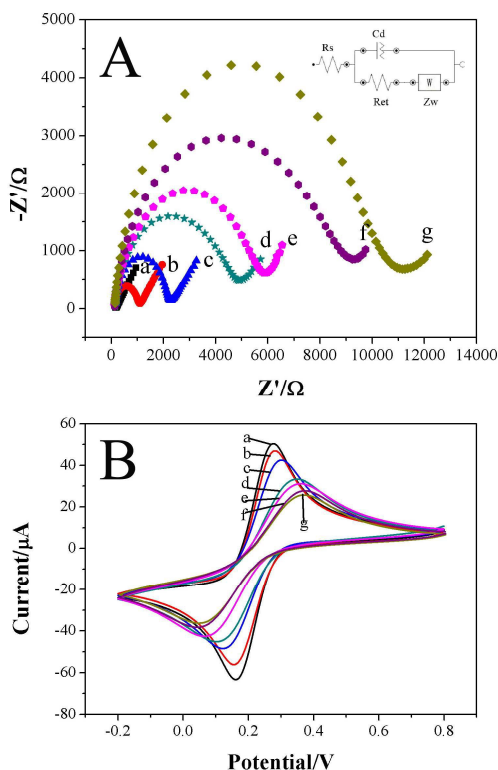


Fig. 3 (A) EIS and (B) CV of different modified electrodes, bare AuE (a), ssDNA/AuE (b), ssDNA/MCH/AuE (c), dsDNA/MCH/AuE (d), dUTP/dsDNA/MCH/AuE (e), BSA/dUTP/dsDNA/MCH/AuE (f) and HRP-SiO₂/BSA/dUTP/dsDNA/MCH/AuE (g). EIS was carried out in a solution containing 10 mM [Fe(CN)₆]³⁻/[Fe(CN)₆]⁴⁻ and 1 M KCl at a potential of 0.2 V (versus Ag/AgCl) from 0.05 Hz to 100 kHz. CV was carried out in a solution containing 10 mM [Fe(CN)₆]³⁻/[Fe(CN)₆]⁴⁻ and 1 M KCl at a scan rate of 100 mV/s from -0.2 V to 0.8 V. Insert showed the equivalent electrical circuit of work electrode.

DNA hybridization detection and electrochemical behavior of HRP-SiO₂ nanoparticles in TMB solution

In order to demonstrate that HRP-SiO₂ nanoparticles could catalyze the TMB, we contrasted the electrochemical signals of PBS and target DNA as hybridization solution, respectively. As shown in Fig. 4A, the reduction peak (curve b, c) of CV of target DNA as hybridization solution were obviously larger than the reduction peak (curve a) of PBS as hybridization solution in TMB solution. Meanwhile, in Fig. 4B the current values of amperometric i-t curve of target DNA were 1384 nA (curve b) and 3590 nA (curve c), but the value of amperometric i-t curve of PBS was visibly smaller 145 nA (curve a) in TMB solution. This is because PBS acted as the hybridization solution without complementary sequence with captured DNA, so there was no hybridization reaction on the modified AuE. The biotin-dUTP

could not be combined on the surface of modified AuE, so the streptavidin-HRP did not connect with DNA and the electrode only produced smaller current signal. Conversely, when the target DNA served as hybridization solution, the biotin-dUTP could pair with the mutant point of target DNA (base A) to fasten on the modified electrode. And then, streptavidin-HRP bonded with the modified electrode by biotin-streptavidin system and produced larger current signal in the TMB solution. And the modified AuE with HRP-SiO₂ nanoparticles (curve c, 3590 nA) produced greater current signal than the AuE with sole HRP (curve b, 1384 nA), implying HRP-SiO₂ nanoparticles had a desired effect of amplification. The experimental result indicated that the prepared sensor was successful.

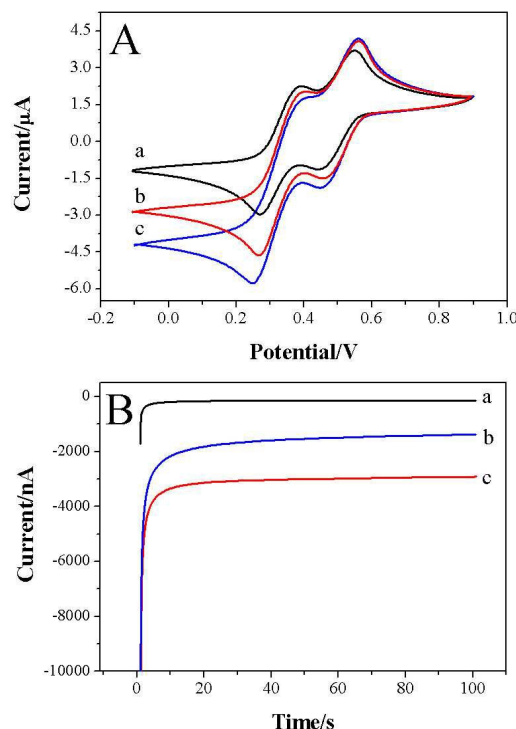


Fig. 4 (A) CV and (B) amperometric i-t curve in TMB solution; (a) PBS as hybridization solution on the modified AuE with HRP-SiO₂ nanoparticles, (b) target DNA with 1 nM as hybridization solution on the modified AuE with HRP and (c) target DNA with 1 nM as hybridization solution on the modified AuE with HRP-SiO₂ nanoparticles (c). CV was carried out at a scan rate of 100 mV/s from -0.1 V to 0.9 V. Amperometric i-t curve was performed with a fixed potential of 100 mV and recorded within 100 s.

Optimization of experimental conditions

The optimum experimental conditions determined the performance of the electrochemical DNA sensor. In order to meet the peak performance of the proposed sensor, we investigated target DNA hybridization temperature, target

DNA hybridization time, DNA polymerase I reaction temperature and DNA polymerase I reaction time for the study. And the optimal experiments were done in the constant concentration (1 nM) of target DNA. Detailed research contents are as follows:

Influence of target DNA hybridization temperature

The temperature of target DNA hybridizing with captured DNA was important parameter which influenced the performance of electrochemical sensor. As shown in Fig. 5A, the current signal increased in the range from 25 °C to 40 °C, and reached the maximum current at 40 °C. After the temperature was greater than 40 °C, the current value gradually decreased. Accordingly, 40 °C was chosen as the optimal temperature of target DNA hybridizing for the experiments.

Influence of target DNA hybridization time

The effect of hybridization time was investigated in the range from 20 min to 120 min. The Fig. 5B showed that the current value increased from 20 min to 60 min, and then tended to level off. This may be because the hybridization reaction was of saturation with the time over 60 min. Thus, 60 min was obtained as the optimal hybridization time.

Influence of DNA polymerase I reaction temperature

The reaction temperature of DNA polymerase I could severely influence the amount of biotin-dUTP immobilized on the modified AuE. As depicted in Fig. 5C, the current value rapidly increased from 25 °C to 37 °C, reached the maximum value at 37 °C and then decreased with the temperature over 37 °C. Therefore, 37 °C was adopted as the optimal reaction temperature of DNA polymerase I.

Influence of DNA polymerase I reaction time

The effect of the reaction time for the current signal was studied at 37 °C. Fig. 5D revealed the influence of DNA polymerase I reaction time from 20 min to 120 min. The current responses increased with the reaction time, and then reached the steady value after more than 60 minutes. So, the reaction time of DNA polymerase I was optimized to be 60 min for the subsequent study.

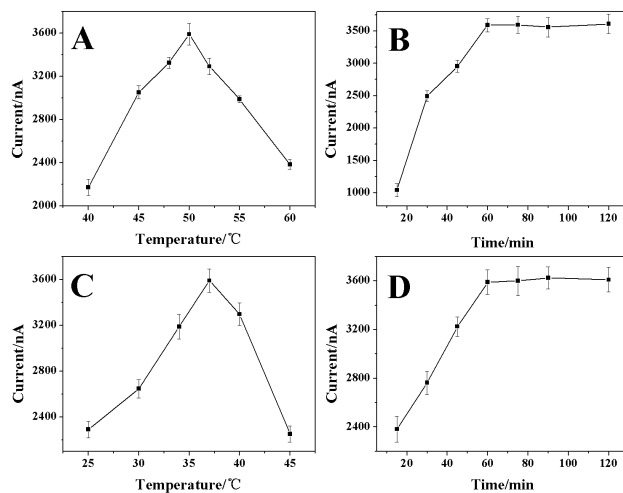


Fig. 5 The influence of different conditions on the modified AuE: (A) target DNA hybridization temperature, (B) target DNA hybridization time, (C) DNA polymerase I reaction temperature and (D) DNA polymerase I reaction time with target DNA of 1 nM. All the experiments were done in the constant concentration (1 nM) of target DNA. All the experiments were detected with a fixed potential of 100 mV and recorded within 100 s in the 500 μ L of TMB solution. Error bars represent the RSD from three independent determinations.

Specificity of the electrochemical DNA sensor

The specificity of the electrochemical DNA sensor was estimated by detecting the mutant K-ras genes and wild K-ras gene with the concentration of 1.0 nM under the optimal experimental conditions. The mutant K-ras genes included target DNA, non-target DNA 1 and non-target DNA 2, the mutation site of which was GAT, GTT and GCT, respectively. As shown in Fig. 6, in TMB solution the current signal of PBS (a), wild K-ras gene (b), non-target DNA 1 (c) and non-target DNA 2 (d) as hybridization solution was 145 nA, 587 nA, 501 nA and 569 nA, respectively. When target DNA (e) acted as the hybridization solution, the signal was 3590 nA and clearly larger than a, b, c and d. The results thoroughly exhibited that the proposed sensor possessed a good discrimination between target DNA and other K-ras genes and provided a research strategy of the gene point mutation detection. The corresponding amperometric i-t curves were shown in Fig. S1.

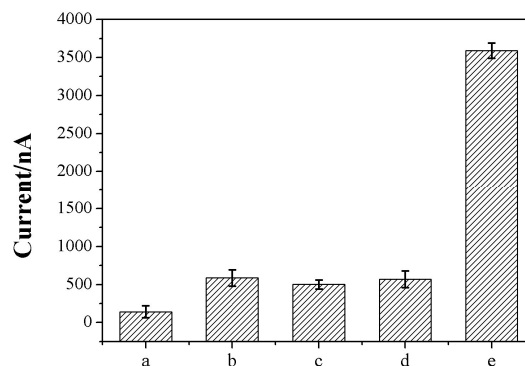


Fig. 6 The histogram of the current signal in TMB solution, PBS (a), wild K-ras gene (b), non-target DNA 1 (c), non-target DNA 2 (d) and target DNA (e) as hybridization solution, respectively. Error bars represent the RSD from three independent determinations.

Quantification detection of target DNA

Fig. 7 showed that the calibration curve of target DNA detection was obtained by employing the proposed electrochemical DNA sensor under optimal conditions. The

response current of the amperometric i-t curve of the proposed sensor showed a good linear to the logarithm of target DNA concentration in the range from 0.001 pM to 1000 pM. The linear regression equation (black square) of the modified AuE with HRP-SiO₂ nanoparticles was $I(nA)=8119.6+516.1\log(C/pM)$ ($R^2=0.9934$). The limit of detection (LOD) of the sensor for target DNA was estimated to be 0.42 fM with three signals to noise ratio. A series of repetitive measurements ($n=8$) of target DNA with 100 pM were used to investigate reproducibility of the proposed approach. The result showed that the relative standard deviation (RSD) was 3.8%, so the reproducibility for target DNA was fine and acceptable. However, the linear regression equation (red circle) of the modified AuE with HRP was $I(nA)=6267.6+411.8\log(C/pM)$ ($R^2=0.9862$). It can be seen that the sensitivity of the modified AuE with HRP-SiO₂ nanoparticles was markedly higher than the modified AuE with sole HRP. The experimental performance of the proposed sensor in the study was compared with the previously reported biosensors for the detection of target DNA. The comparative data were detailedly listed in the Table S1 and revealed that the proposed DNA sensor has some advantages: i) the application of DNA polymerase I improved the selectivity and specificity of the proposed electrochemical DNA sensor; ii) the introduction of SiO₂ nanoparticles obviously amplified the electrochemical signal to enhance sensitivity of the sensor; iii) the treatment process of the working electrode is very simple and do not need special treatment; iv) the proposed DNA sensor was successfully applied for the analysis of mixture sample with target DNA, non-target DNA 1, non-target DNA 2 and wild K-ras gene. And as can be seen from Table S1, the sensor has a wider linear rang and a lower limit of detection.

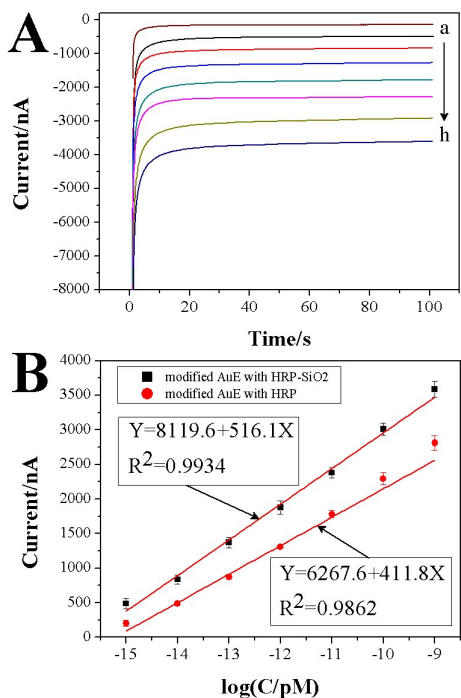


Fig. 7 (A) Amperometric i-t curves of target DNA different concentrations (from a to h: 0, 0.001 pM, 0.01 pM, 0.1 pM, 1 pM, 10 pM, 100 pM, 1000 pM) on the modified AuE with HRP-SiO₂ nanoparticles. (B) The linear relation between the response current value and the logarithm of target DNA concentration; Black Square and red circle stand for the modified AuE with HRP-SiO₂ nanoparticles and HRP, respectively. Error bars represent the RSD from three independent determinations.

Analysis of mixture sample

The majority of clinical samples are the mixture with target DNA and other similar DNA, so we designed the experiment quantitatively analyzes the mixture sample containing target DNA, non-target DNA 1, non-target DNA 2 and wild K-ras gene in the study. Non-target DNA 1, non-target DNA 2 and wild K-ras gene were as interference background in the hybridization solution. As shown in Fig. 8, the current value was also proportional to the logarithm of the target DNA concentration from 0.01 pM to 100 pM when the concentration of non-target DNA 1, non-target DNA 2 and wild K-ras gene was 0.1 nM. The ratio of target DNA to other similar DNA (non-target DNA 1, non-target DNA 2 and wild K-ras gene) was from 1:1 to 1:10000. The linear regression equation is $I(nA)=8756.5+559.7\log(C/pM)$ ($R^2=0.9871$). The results showed that the developed approach could quantitatively analyze the target DNA in the mixture sample and be used as a novel method to detect the K-ras gene.

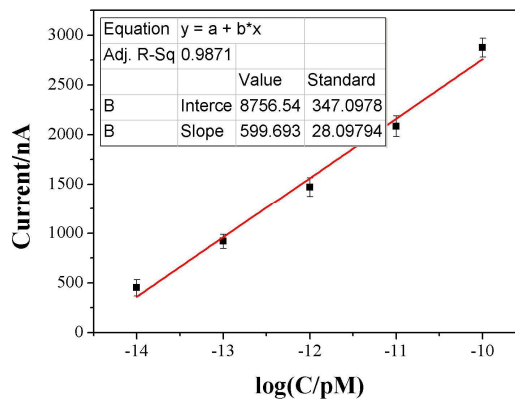


Fig. 8 The linear relation between the response current value and the logarithm of target DNA concentration in the mixture sample containing other similar DNA (non-target DNA 1, non-target DNA 2 and wild K-ras gene). The concentration of non-target DNA 1, non-target DNA 2 and wild K-ras gene was 0.1 nM. Error bars represent the RSD from three independent determinations.

Conclusions

In the present study, a novel electrochemical DNA sensor was developed for the detection of point mutation of K-ras gene. It was ingenious to combine DNA polymerase β with HRP-SiO₂ nanoparticles. DNA polymerase β was used for linking U with A by base pairing, which ensured the proposed sensor had excellent specificity. HRP-SiO₂ nanoparticles could amplify the response signal to make the sensor possess high sensitivity. And the proposed method had the advantage of wide linear range (0.001 pM~100 pM) and low LOD (0.42 fM). Meanwhile, the proposed DNA sensor could still detect the target DNA in the presence of other similar DNA (non-target DNA 1, non-target DNA 2 and wild K-ras gene) as high as 0.1 nM and had a good linear relation. The detecting techniques for the detection of point mutation of gene provided a good basis and a promising platform, which will be employed to detect the clinical genomic sample about single base mutation.

Acknowledgements

We are thankful for financial support from the financial support of the Science and technology project of the Education Department of Fujian Province (JA15445), the National High Technology and Development of China (863 Project: 2012AA022604) and the National Natural Science Foundation of China (81571613, 81572442, 21405016, 21275028).

Notes and references

‡ Footnotes relating to the main text should appear here. These might include comments relevant to but not central to the matter under discussion, limited experimental and spectral data, and crystallographic data.

§

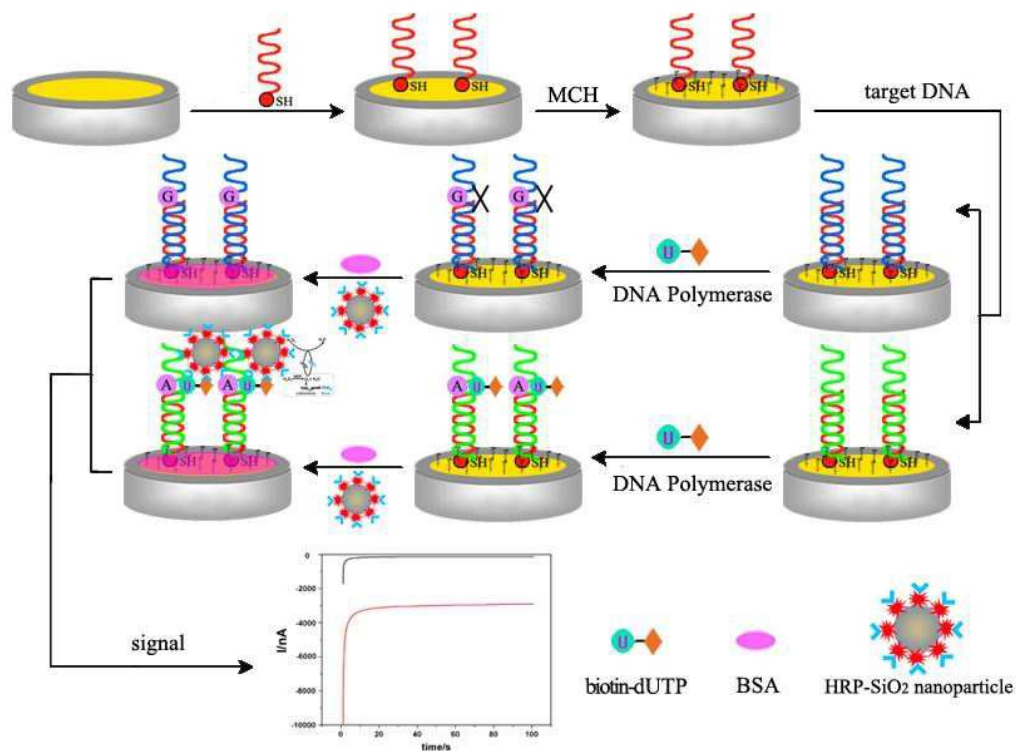
§§

etc.

- 1 D. Yadav and A.B. Lowenfels, *Gastroenterology*, 2013, **144**, 1252-1261.
- 2 A. Vincent, J. Herman, R. Schulick, R.H. Hruban and M. Goggins, *Lancet*, 2011, **378**, 607-620.
- 3 G. Lucio, T. Paola, M. Marina, C. Riccardo and M. Domenico, *Pancreas*, 2001, **22**, 210-213.
- 4 M. Loos, J. Kleeff, H. Friess and M.W. Büchler, *Ann. NY. Acad. Sci.*, 2008, **1138**, 169-180.
- 5 Q.C. Liu, A.L. Liu, S.H. Weng, G.X. Zhong, J.F. Liu, X.H. Lin, J.H. Lin and X.H. Chen, *Int. J. Nanomed*, 2011, **6**, 2933-2939.
- 6 R.H. Hruban, N.V. Adsay, J. Albores-Saavedra, C. Compton, E.S. Garrett, S.N. Goodman, S.E. Kern, D.S. Klimstra, G. Kloppel, D.S. Longnecker, J. Luttges and G.J. Offerhaus, *Am. J. Surg. Pathol.*, 2001, **25**, 579-589.
- 7 T. Deramaudt and A.K. Rustgi, *BBA-Rev Cancer*, 2005, **1756**, 97-101.
- 8 R.H. Hruban, M. Goggins, J. Parsons and S.E. Kern, *Clin. Cancer Res.*, 2000, **6**, 2969-2972.
- 9 S.T. Kim, D.H. Lim, K.T. Jang, T. Lim, J. Lee, Y.L. Choi, H.L. Jang, J.H. Yi, K.K. Baek, S.H. Park, Y.S. Park, H.Y. Lim, W.K. Kang and J.O. Park, *Mol. Cancer Ther.*, 2011, **10**, 1993-1999.
- 10 D.H. Li, K.P. Xie and R. Wolff, *Lancet*, 2004, **363**, 1049-1057.
- 11 M. Hashimoto, F. Barany and S.A. Soper, *Biosens. Bioelectron.*, 2006, **21**, 1915-1923.
- 12 A.T. Christian, M.S. Pattee, C.M. Attix, B.E. Reed, K.J. Sorensen and J.D. Tucker, *P. Natl. Acad. Sci. USA*, 2001, **98**, 14238-14243.

- 13 E. Paleček, M. Masařík, R. Kizek, D. Kuhlmeier, J. Hassmann and J. Schülein, *Anal. Chem.*, 2004, **76**, 5930-5936.
- 14 F. Patolsky, A. Lichtenstein and I. Willner, *Nat. Biotechnol.*, 2001, **19**, 253-257.
- 15 H.J. Fan, X.L. Wang, F. Jiao, F. Zhao, Q.J. Wang, P. He and Y.Z. Fang, *Anal. Chem.*, 2013, **85**, 6511-6517.
- 16 J. Zhang, S.P. Song, L.H. Wang, D. Pang and C.H. Fang, *Nat. Protoc.*, 2007, **2**, 2888-2895.
- 17 L.Q. Lin, S.H. Weng, C.F. Zhao, Q.C. Liu, A.L. Liu and X.H. Lin, *Electrochim. Acta*, 2013, **108**, 808-813.
- 18 L.Q. Lin, A.L. Liu, C.F. Zhao, S.H. Weng, Y. Lei, Q.C. Liu, X.H. Lin and Y.Z. Chen, *Biosens. Bioelectron.*, 2013, **42**, 409-414.
- 19 W. Shen, H.M. Deng, Y.Q. Ren and Z.Q. Gao, *Biosens. Bioelectron.*, 2013, **43**, 165-172.
- 20 Y. Chen, M.L. Yang, Y. Xiang, R. Yuan and Y.Q. Chai, *Anal. Chim. Acta*, 2013, **796**, 1-6.
- 21 C.F. Zhao, S.F. Yang, L.Q. Liu, S.H. Wang, Q.C. Liu, A.L. Liu and X.H. Lin, *Sensor Actuat B-Chem.*, 2016, **223**, 946-951.

Graphical and textual abstract



We successfully developed an electrochemical DNA sensor for the precise detection of K-ras gene point mutation. The proposed sensor was based on DNA replication, which fully employed the 5' → 3' polymerization activity of DNA polymerase I and the principle of base pairing. The biotin-dUTP only linked with the base A, instead of base G. And then, the streptavidin-HRP-SiO₂ nanoparticles combining with the biotin-dUTP on the modified electrode produced the current signal in the TMB solution. The streptavidin-HRP-SiO₂ nanoparticles had the effect of amplified signal. Hence, the sensitivity and selectivity of the proposed

sensor were observably enhanced, comparison with the previously reported DNA sensors. The response current of the amperometric *i-t* curve of the prepared sensor showed a good linear correlation with the logarithm of target DNA concentration in the range from 0.001 pM to 1000 pM with the limit of detection of 0.42 fM. And the current value was also proportional to the logarithm of target DNA concentration from 0.01 pM to 100 pM when the hybridization solution contained other mutant K-ras genes and wild K-ras gene. Thus, this proposed approach provided the good basis and a promising platform that the mutant K-ras gene in the clinical genomic sample can be directly detected.